

Magnetotropic Response in Ruthenium Chloride

Ipsita Mandal*

Institute of Nuclear Physics, Polish Academy of Sciences, 31-342 Kraków, Poland

We consider the exchange couplings present in an effective Hamiltonian of α -RuCl₃, known as the K- Γ model. This material has a honeycomb lattice, and is expected to be a representative of the Kitaev materials (which can realize the 2d Kitaev model). However, the behaviour of RuCl₃ shows that the exchange interactions of the material are not purely Kitaev-like, especially because it has an antiferromagnetic ordering at low temperatures and under low strengths of an externally applied magnetic field. Fitting the data obtained from the measurements of the magnetotropic coefficient (the thermodynamic coefficient associated with magnetic anisotropy), reported in *Nature Physics* 17, 240–244 (2021), we estimate the values of the exchange couplings of the effective Hamiltonian. The fits indicate that the Kitaev couplings are subdominant to the other exchange couplings.

Keywords: α -RuCl₃; magnetotropic coefficient; K- Γ model

I. INTRODUCTION

Spin-orbit coupling (SOC) assisted (spin $j = 1/2$) Mott insulators, exhibiting bond-directional exchange interactions, are expected to exhibit unconventional quantum magnetic phases like spin liquids [1, 2], predicted by the two-dimensional (2d) Kitaev model [3] on honeycomb lattice. These putative quantum spin liquids are dubbed as “Kitaev spin liquids” (KSLs) [4–8], and the materials expected to show such behaviour are called Kitaev materials. Compounds like honeycomb iridates and α -RuCl₃ have been identified as candidate Kitaev materials. The hallmark feature of a Kitaev material is that the Kitaev coupling is the dominant exchange coupling. However, the behaviour of RuCl₃ shows that the exchange interactions of the material are not purely Kitaev-like. In this paper, we will address the unresolved question regarding what the possible exchange couplings in α -RuCl₃ [7–11] could be – for example, what the dominant terms in the effective spin Hamiltonian are, and whether we can estimate the values of these coupling constants.

At low energies, experiments [12–14] show signatures consistent with a zig-zag antiferromagnet (AFM) background (also consistent with *ab initio* calculations [9, 15, 16]), while indicating the existence of an unconventional quantum magnetic phase, which could be the much sought-after KSL induced by a finite magnetic field. Exact numerical diagonalization methods to investigate the data from dynamical spin structure factors, and that from heat capacity measurements [17, 18], found that off-diagonal interactions are dominant rather than Kitaev interactions [19]. On the other hand, other computational papers [7, 9, 10, 20] report that Kitaev terms are the dominant ones. We focus on the results from resonant torsion magnetometry experiments [21], which can measure the magnetotropic coefficient $k \equiv \frac{\partial^2 F}{\partial \theta^2}$ at temperature \mathcal{T} . Here, $F = -\beta^{-1} \ln Z$ is the free energy, $\beta = \frac{1}{k_B \mathcal{T}}$, and θ is the angle between the applied magnetic field \mathbf{B} and the c -axis of the crystal. Using a simple Hamiltonian with a dominant paramagnetic term, we will show that we can fit the data obtained from the measurements of the magnetotropic coefficient, and the fits correspond to the Kitaev terms being subdominant in the so-called K- Γ model.

II. MODEL

Due to the presence of on-site SOC, the effective magnetic field components along the spin projections are given by:

$$\tilde{B}_\alpha \equiv B_\gamma D_{\gamma\alpha}, \quad [D] = \mathcal{A} \mathbb{1}_{3 \times 3} + \begin{pmatrix} 0 & \mathcal{B} & \mathcal{B} \\ \mathcal{B} & 0 & \mathcal{B} \\ \mathcal{B} & \mathcal{B} & 0 \end{pmatrix}, \quad (2.1)$$

where the form of $[D]$ has been fixed by the C_3 and C_2 rotation symmetries [22] of P3₁12, constraining it to have \mathcal{A} and \mathcal{B} as the only two independent components (see Appendix A). In the abc -coordinate system, $[D]$ is rotated to take the diagonal form, $\text{diag}\{g_a, g_a, g_c\}$, where the g -factors are given by:

$$\tilde{g}_a = \frac{k_B g_a}{\mu_B}, \quad \tilde{g}_c = \frac{k_B g_c}{\mu_B}, \quad g_a = \mathcal{A} - \mathcal{B}, \quad g_c = \mathcal{A} + 2\mathcal{B}, \quad (2.2)$$

such that $k_B = 1.38064852 \times 10^{-23} \text{ J/K}$ and $\mu_B = 9.274 \times 10^{-24} \text{ J/T}$. The SOC thus forces the leading order paramagnetic term in our model Hamiltonian to be $H_0 = - \sum_{\alpha=\{x,y,z\}} \tilde{B}_\alpha \sigma_j^\alpha$, rather than $\left(- \sum_{\alpha=\{x,y,z\}} B_\alpha \sigma_j^\alpha \right)$. We note that the Hamiltonian has the

* ipsita.physics@gmail.com

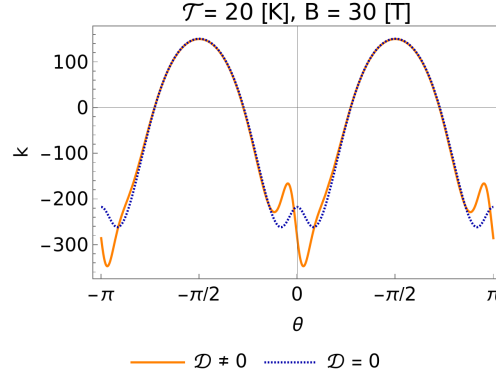


FIG. 1. Plots of k versus θ computed from our theoretical model, where the orange curve represents the one obtained with the best-fit parameters for the ($\mathcal{T} = 20$ K, $B = 30$ T) data-set, whereas the dotted blue curve has been drawn using those same parameters, except that we have set $\mathcal{D} = 0$. This clearly shows that we can never get an asymmetric spike around $\theta = 0$ without an asymmetric off-diagonal Γ term, which represents DM interactions.

units of $g \mu_B \boldsymbol{\sigma} \cdot \mathbf{B}$ ($\boldsymbol{\sigma}$ is the dimensionless spin-1/2 vector operator), such that $\frac{g \mu_B \boldsymbol{\sigma} \cdot \mathbf{B}}{k_B T}$ is dimensionless (because we have factors like $e^{-\beta H}$). Hence, \mathcal{A} and \mathcal{B} have units of K/T .

Following the arguments above, the physics of a honeycomb lattice, restricted to nearest-neighbor interactions, and subjected to an external magnetic field \mathbf{B} , can be captured by a Hamiltonian of the form:

$$H = H_0 + V, \quad H_0 = - \sum_{\alpha=\{x,y,z\}} \tilde{B}_\alpha \sigma_j^\alpha, \quad V = \sum_{\gamma=\{x,y,z\}} \sum_{\langle jk \rangle_{\gamma\text{-links}}} J_{\alpha\beta}^\gamma \sigma_j^\alpha \sigma_k^\beta, \quad (2.3)$$

where H_0 is the leading order part for large B , and V is the subleading part. The second summation in V runs over nearest-neighbour spins at sites j and k , coupled by a bond along the $\gamma = (x, y, z)$ direction. Furthermore, $J_{\alpha\beta}^\gamma$ is the coupling constant (for a given value of α , β , and γ), σ_j^μ ($\mu = x, y, z$) is the Pauli spin matrix representing the spin-1/2 operator on site j , projected along the μ -axis. The spins are located on the vertices of the honeycomb lattice and $\langle jk \rangle$ denotes the labels of the nearest-neighbour spins. For a hexagonal lattice, there are three different kinds of bonds that can be grouped according to their alignments (see Fig. 3 of Ref. [3]) – vertical bonds (which we label as z -links), bonds with positive slope (which we label as x -links), and bonds with negative slope (which we label as y -links). Hence, a given site j is connected to three other sites by these three different types of links, denoted by γ . In other words, the links are not oriented along the 3d orthogonal Cartesian coordinate directions, but each γ -value denotes the orientation of the bond we are referring to.

The parameters $J_{\alpha\beta}^\gamma$ are obtained from the K- Γ model, where K stands for the Kitaev term of the 2d Kitaev model [3], and Γ represents the off-diagonal exchange interactions [7, 8, 10, 20], as follows:

$$H_K = \kappa \left(\sum_{\langle j,k \rangle_{x\text{-links}}} \sigma_j^x \sigma_k^x + \sum_{\langle j,k \rangle_{y\text{-links}}} \sigma_j^y \sigma_k^y + \sum_{\langle j,k \rangle_{z\text{-links}}} \sigma_j^z \sigma_k^z \right),$$

$$H_\Gamma = \Gamma \left[\sum_{\langle j,k \rangle_{x\text{-links}}} (\sigma_j^y \sigma_k^z + \sigma_j^z \sigma_k^y) + \sum_{\langle j,k \rangle_{y\text{-links}}} (\sigma_j^z \sigma_k^x + \sigma_j^x \sigma_k^z) + \sum_{\langle j,k \rangle_{z\text{-links}}} (\sigma_j^x \sigma_k^y + \sigma_j^y \sigma_k^x) \right]$$

$$+ \mathcal{D} \left[\sum_{\langle j,k \rangle_{x\text{-links}}} (\sigma_j^y \sigma_k^z - \sigma_j^z \sigma_k^y) + \sum_{\langle j,k \rangle_{y\text{-links}}} (\sigma_j^z \sigma_k^x - \sigma_j^x \sigma_k^z) + \sum_{\langle j,k \rangle_{z\text{-links}}} (\sigma_j^x \sigma_k^y - \sigma_j^y \sigma_k^x) \right]. \quad (2.4)$$

Here κ is the strength of the Kitaev term, and Γ represents the off-diagonal exchange interaction strengths. The parameters Γ and \mathcal{D} represent the symmetric and antisymmetric parts of the off-diagonal terms.

If the trivial paramagnetic term H_0 dominates the response of the system to the external magnetic field, we can perform a thermodynamic expansion of the partition function [23], as reviewed in Appendix B. Then the partition function, corrected to leading order, evaluates to:

$$\mathcal{Z}(T) = \left[2 \cosh(\beta \tilde{B}) \right]^{2N_c} \left[1 + \beta N_c \sum_{\gamma, \alpha', \lambda'} J_{\alpha'\lambda'}^\gamma \frac{\sinh(\beta \tilde{B}_{\alpha'}) \sinh(\beta \tilde{B}_{\lambda'})}{\cosh^2(\beta \tilde{B})} \right], \quad \text{where } \tilde{B} = \sqrt{\sum_{\alpha} \tilde{B}_\alpha \tilde{B}_\alpha}, \quad (2.5)$$

where N_c is the number of unit cells (or, half the number of honeycomb lattice sites) in the system. It turns out that this simple model can indeed explain the experimental data, to a high degree of precision.

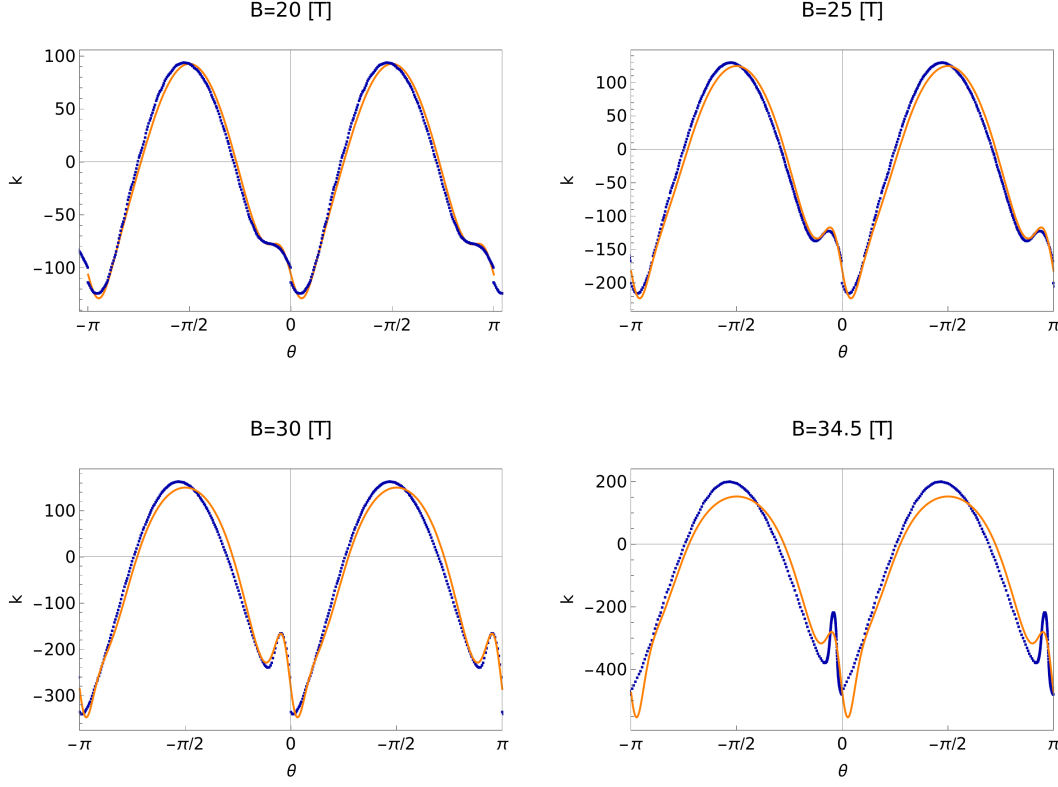


FIG. 2. The data-sets for k versus θ (in radians) at $\mathcal{T} = 20 K$ for various values of the applied magnetic field strength B (in units of Tesla). We have represented the experimental data-points in blue, and the best-fit curves in orange.

$B = 20 T$	Estimate	Standard Error	Confidence Interval
κ	54.4	2.37	{52.1, 56.7}
Γ	102	6.09	{96.8, 108}
\mathcal{D}	-9.60	0.629	{-10.2, -8.98}
g_a	4.00	0.137	{3.87, 4.13}
g_c	1.79	0.0984	{1.70, 1.89}
ζ	2.00	0.0736	{1.93, 2.07}
η	-9.38	0.150	{-9.53, -9.23}

$B = 25 T$	Estimate	Standard Error	Confidence Interval
κ	74.6	1.32	{73.3, 75.9}
Γ	133	8.80	{125, 142}
\mathcal{D}	-13.9	0.866	{-14.7, -13.1}
g_a	4.00	0.124	{3.88, 4.12}
g_c	1.52	0.0677	{1.46, 1.59}
ζ	2.00	0.071	{1.93, 2.07}
η	-24.4	0.281	{-24.7, -24.2}

$B = 30 T$	Estimate	Standard Error	Confidence Interval
κ	95.8	1.46	{94.4, 97.3}
Γ	152	9.46	{143, 161}
\mathcal{D}	-15.8	0.841	{-16.6, -15.0}
g_a	4.00	0.118	{3.88, 4.11}
g_c	1.26	0.0486	{1.21, 1.30}
ζ	2.00	0.0687	{1.93, 2.07}
η	-50.1	0.507	{-50.6, -49.6}

$B = 34.5 T$	Estimate	Standard Error	Confidence Interval
κ	85.5	2.90	{82.6, 88.3}
Γ	156	28.7	{128, 184}
\mathcal{D}	-20.3	3.31	{-23.5, -17.1}
g_a	4.00	0.276	{3.73, 4.27}
g_c	1.20	0.122	{1.08, 1.32}
ζ	2.00	0.145	{1.86, 2.14}
η	-88.8	1.42	{-90.2, -87.4}

TABLE I. The table shows the fitting of parameters at 67% confidence level, for the k versus θ data-set. Here, B and $\{\kappa, \Gamma, \mathcal{D}\}$ are in units of T , $\{g_a, g_c\}$ are in units of K/T , ζ is dimensionless, and η has the same unit as k .

III. FITTING THE DATA

According to some papers in the literature [9, 24], the point-group symmetry of the Ru-Ru links is C_{2h} in a $C/2m$ unit cell, and hence the antisymmetric Dzyaloshinskii-Moriya (DM) exchange is zero. Because spin is an axial vector itself, the non-zero antisymmetric part of $J_{\alpha\beta}^{\gamma}$ is equivalent to $\mathbf{P} \cdot (\mathbf{S} \times \mathbf{S})$ term where \mathbf{P} is a polar vector. So in order to have a DM term in exchange, the chemical environment of the Ru-Ru bond must allow for a polar vector. In the undistorted honeycomb lattice, such a polar vector is prohibited by symmetry. It is non-zero for next-nearest neighbor exchange links (even in the undistorted case) [25] or if Cl

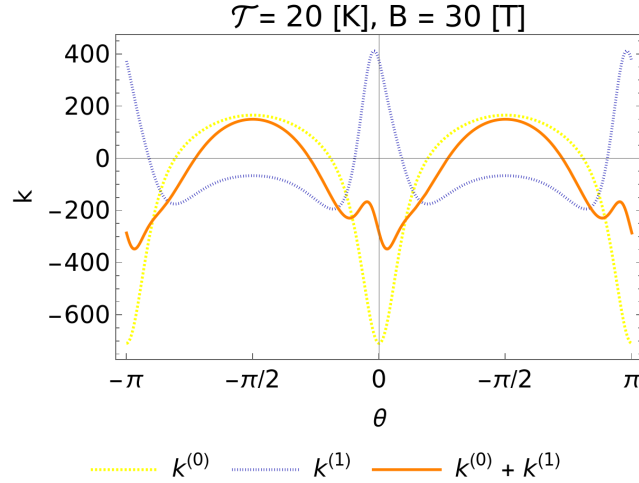


FIG. 3. We have plotted three curves corresponding to (1) leading order expression $k^{(0)}$; (2) first order correction $k^{(1)}$; and (3) $k^{(0)} + k^{(1)}$, as functions of θ , which have been computed from our theoretical model, using the best-fit parameters for the ($T = 20 K$, $B = 30 T$) data-set. These three curves are shown in dashed yellow, dotted blue, and orange, respectively.

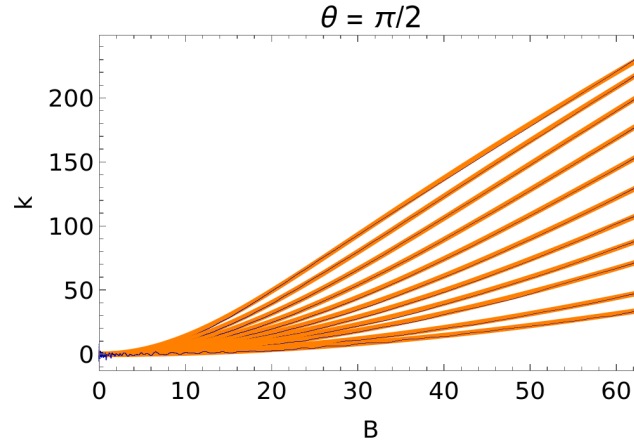


FIG. 4. The data-sets for k versus B (in units of Tesla) at $\theta = \pi/2$ for temperatures ranging from $T = 30 K$ to $T = 150 K$ at intervals of $10 K$. The topmost curve represents the $30 K$ data, whereas the lowermost curve represents the $150 K$ data. We have represented the experimental data-points in blue, and the best-fit curves in orange.

octahedra are distorted. However, the peak shapes in the k versus θ data (and the behavior in a broader angular range around it) are not symmetric around the c -axis, *i.e.*, $k(\theta) - k(-\theta) \neq 0$. We find that this behavior is possible only if we allow the antisymmetric DM term, which points to a distorted octahedra, leading to a deviation from the assumed crystal symmetries. This is shown in Fig. 1, where we show the plots for $k(\theta)$ computed from our model, with the parameter values taken from the best-fit parameters of the $B = 30 T$ data (except that we set $\mathcal{D} = 0$ for the orange curve).

The expressions for F and k depend on the polar angle θ , but not on the azimuthal angle ϕ . We fit the data-sets for four different values of the applied magnetic field strength B , using “NonlinearModelFit” of Mathematica. The data-sets for $B \leq 15 T$ are not considered as they are either close to or within the AFM phase. Since the scaling and absolute shift of each data-set are uncertain, we include two more parameters, namely, “ ζ ” and “ η ” corresponding to the unknown scale and shift. The experimental data and the fitted functions are shown in Fig. 2. The confidence intervals for all the parameters at 67% confidence level are shown in Table I.

We also fit the k versus B data available for $\theta = \pi/2$. One can check that the correction terms from $J_{\alpha\beta}^{\gamma}$ hardly affect the regions around $\theta = \pi/2$ (see Fig. 3). They have the most visible impact only around the $\theta = 0$ and $\theta = \pi$ regions. Hence, the fitting process keeping the first order correction makes the parameters indeterminate. However, if we fit only with the zeroth order expression, we get excellent values for g_a and g_c . We also need to include a parameter “ η ” to account for the uncertainty in the absolute shift of the data-set for each temperature value. These fits are shown in Fig. 4. The data-sets for temperatures $T \leq 20 K$ are not considered as each of them has a considerable region within the AFM phase in the low B ranges, which cannot be fitted by the functional forms meant for the paramagnetic phase. The confidence intervals for g_a , g_c , and η , at 67% confidence level, are shown in Table II.

$\mathcal{T} = 30 K$	Estimate	Standard Error	Confidence Interval
g_a	2.43	0.00172	{2.43, 2.44}
g_c	1.20	0.00148	{1.2, 1.20}
η	0.000131	0.0158	{-0.0152, 0.0155}

$\mathcal{T} = 40 K$	Estimate	Standard Error	Confidence Interval
g_a	2.46	0.000785	{2.46, 2.46}
g_c	1.24	0.000738	{1.24, 1.24}
η	0.000267	0.00700	{-0.00655, 0.00709}

$\mathcal{T} = 50 K$	Estimate	Standard Error	Confidence Interval
g_a	2.42	0.000581	{2.42, 2.42}
g_c	1.23	0.000600	{1.23, 1.23},
η	0.00822	0.00473	{0.00362, 0.0128}

$\mathcal{T} = 60 K$	Estimate	Standard Error	Confidence Interval
g_a	2.34	0.000456	{2.34, 2.34}
g_c	1.20	0.000518	{1.20, 1.20}
η	0.00592	0.00310	{0.00290, 0.00894}

$\mathcal{T} = 70 K$	Estimate	Standard Error	Confidence Interval
g_a	2.28	0.000920	{2.28, 2.28}
g_c	1.20	0.00113	{1.20, 1.20}
η	0.00923	0.00490	{0.00446, 0.0140}

$\mathcal{T} = 80 K$	Estimate	Standard Error	Confidence Interval
g_a	2.20	0.00158	{2.2, 2.2}
g_c	1.20	0.00204	{1.20, 1.20}
η	0.0452	0.00637	{0.039, 0.0514}

$\mathcal{T} = 90 K$	Estimate	Standard Error	Confidence Interval
g_a	2.12	0.00235	{2.12, 2.12}
g_c	1.20	0.00316	{1.20, 1.20}
η	-0.0124	0.00691	{-0.0191, -0.00565}

$\mathcal{T} = 100 K$	Estimate	Standard Error	Confidence Interval
g_a	2.03	0.00351	{2.03, 2.03}
g_c	1.20	0.00481	{1.20, 1.20}
η	0.043	0.00740	{0.0358, 0.0503}

$\mathcal{T} = 110 K$	Estimate	Standard Error	Confidence Interval
g_a	1.94	0.00531	{1.94, 1.95}
g_c	1.20	0.00732	{1.19, 1.201}
η	-0.00637	0.0078	{-0.014, 0.00123}

$\mathcal{T} = 130 K$	Estimate	Standard Error	Confidence Interval
g_a	1.79	0.0111	{1.78, 1.80}
g_c	1.20	0.0151	{1.18, 1.21}
η	-0.0081	0.00815	{-0.016, -0.000166}

$\mathcal{T} = 150 K$	Estimate	Standard Error	Confidence Interval
g_a	1.76	0.0953	{1.66, 1.85}
g_c	1.287	0.122	{1.17, 1.41}
η	-0.00276	0.0385	{-0.0403, 0.0347}

TABLE II. The table shows the fitting of parameters at 67% confidence level, for the k versus B data-set. Here, temperature \mathcal{T} is in units of Kelvin (K), $\{g_a, g_c\}$ are in units of K/T , and η has the same unit as k .

IV. SUMMARY AND OUTLOOK

Let us discuss some other possibilities which might be responsible for causing the asymmetry in the spike around $\theta = 0$ in the k versus θ data. Firstly, in the experimental set-ups, the path along which the sample is rotated in the external magnetic field to change θ , may deviate from a great circle, leading to an uncertainty of upto 10° . However, incorporating these deviations, the theoretical curves do not show the desired asymmetry [26]. Secondly, the K - Γ Hamiltonian (even without DM, distortion, misalignment of rotation etc.) lacks mirror reflection symmetry. Therefore, magnetotropic coefficients (or free energy) are different for applied magnetic fields, \mathbf{B} and \mathbf{B}' , that are related by a mirror reflection in honeycomb plane. Such asymmetry is artificially removed in low-order perturbation theory. This is directly analogous to accidental symmetries of the standard model (such as separate conservation of baryon and lepton number) that only exist in the lowest order of expansion in inverse GUT scale. It is a general phenomenon – low orders in perturbation theory tend to accidentally “restore” some of the symmetries of the Hamiltonian. In the Kitaev model, the lowest order perturbation expansion in magnetic field [3] is symmetric (with respect to mirror- ab -plane) – one needs to go to higher orders in B to see the asymmetry of the Hamiltonian. The same might be true for the thermodynamic perturbative expansion. By going to higher orders (second, or maybe third order), the asymmetric character of the Hamiltonian may eventually show up. However, such higher order computations are beyond the scope of this paper.

Our best-fit parameters show that the Kitaev terms are subdominant to the Γ (and \mathcal{D}) terms. In fact, the large Γ value contrasts with the expectation so far [7, 9, 10, 20] that α - RuCl_3 is a “Kitaev model material”. It has also been predicted [9, 20, 27] in those models (including a small Heisenberg term) that the ratio $g_c/g_a \simeq 0.4 - 0.5$. Our results (see Fig. I) are close to these results, although we should remember that our model differs from theirs.

V. ACKNOWLEDGMENTS

We thank Michael J. Lawler for suggesting the problem. We are also grateful to Brad Ramshaw, Arkady Shekhter, and Kimberly Modic for insightful discussions.

Appendix A: Choice of coordinate system and crystal symmetries

We choose a coordinate system such that the plane of the honeycomb lattice is described by three in-plane vectors $\mathbf{r}_1 = (0, 1, -1)$, $\mathbf{r}_2 = (-1, 1, 0)$, $\mathbf{r}_3 = (-1, 0, 1)$, as they lie on the plane formed by cutting the three points: $(1, 0, 0)$, $(0, 1, 0)$ and $(0, 0, 1)$. Then the perpendicular vector is $\mathbf{r}_\perp = (1, 1, 1)/\sqrt{3}$ and we choose the in-plane direction as $\mathbf{r}_2/\sqrt{2}$, giving $\frac{\mathbf{B}}{B} = \frac{\cos\theta(1,1,1)}{\sqrt{3}} + \frac{\sin\theta(-1,1,0)}{\sqrt{2}}$, with the magnetic field making an angle θ with the c -axis. Let us also define the a -axis along the line joining $(1, 1, 1)/3$ and $(1, 0, 0)$, such that the projection of \mathbf{B} on the ab -plane makes an angle ϕ with the a -axis.

Given a unit vector \mathbf{u} , the matrix for a rotation by an angle of ϕ about an axis in the direction of \mathbf{u} is:

$$R(\mathbf{u}, \phi) = \begin{pmatrix} \cos\phi + u_x^2(1 - \cos\phi) & u_x u_y(1 - \cos\phi) - u_z \sin\phi & u_x u_z(1 - \cos\phi) + u_y \sin\phi \\ u_y u_x(1 - \cos\phi) + u_z \sin\phi & \cos\phi + u_y^2(1 - \cos\phi) & u_y u_z(1 - \cos\phi) - u_x \sin\phi \\ u_z u_x(1 - \cos\phi) - u_y \sin\phi & u_z u_y(1 - \cos\phi) + u_x \sin\phi & \cos\phi + u_z^2(1 - \cos\phi) \end{pmatrix}. \quad (\text{A1})$$

Now the crystal symmetry allows invariance under a C_3 rotation about \mathbf{r}_\perp , which corresponds to invariance under the rotation matrix:

$$R(\mathbf{r}_\perp, 2\pi/3) = \begin{pmatrix} 0 & 0 & 1 \\ 1 & 0 & 0 \\ 0 & 1 & 0 \end{pmatrix}. \quad (\text{A2})$$

For C_2 rotation about \mathbf{r}_1 , we have:

$$R\left(\frac{\mathbf{r}_1}{\sqrt{2}}, \pi\right) = \begin{pmatrix} -1 & 0 & 0 \\ 0 & 0 & -1 \\ 0 & -1 & 0 \end{pmatrix}. \quad (\text{A3})$$

Due to on-site spin-orbit coupling, the leading order paramagnetic term in our model is given by $H_0 = -\sum_{\alpha=\{x,y,z\}} \tilde{B}_\alpha \sigma_j^\alpha$, rather than $\left(-\sum_{\alpha=\{x,y,z\}} B_\alpha \sigma_j^\alpha\right)$, where $\tilde{B}_\alpha \equiv B_\gamma D_{\gamma\alpha}$. We still have the C_3 and C_2 rotation symmetries of P3₁12 [22] to be satisfied, which implies that:

$$[B]^T [D] [\sigma] = (R[B])^T [D] R[\sigma] \Rightarrow D = R^T [D] R, \quad (\text{A4})$$

where R has been defined in Eq. (A2). Then, $R(\mathbf{r}_\perp, 2\pi/3)$ and $R\left(\frac{\mathbf{r}_1}{\sqrt{2}}, \pi\right)$ restrict $[D]$ to have only two independent components, namely \mathcal{A} and \mathcal{B} , such that

$$[D] = \mathcal{A} \mathbb{1}_{3 \times 3} + \begin{pmatrix} 0 & \mathcal{B} & \mathcal{B} \\ \mathcal{B} & 0 & \mathcal{B} \\ \mathcal{B} & \mathcal{B} & 0 \end{pmatrix}. \quad (\text{A5})$$

Appendix B: Thermodynamic expansion of the K- Γ model in the large magnetic field limit

We perform a thermodynamic expansion of the K- Γ model in the large magnetic field limit, following the methods describe in Ref. 23, which are applicable when we are interested in the thermodynamic properties at finite temperature. We review this perturbation expansion when the Hamiltonian can be written as $H = H_0 + \lambda V$, where H_0 is the leading order part for large B , and λ is the perturbative expansion parameter, with V being the subleading part.

We are interested in the thermodynamic properties at finite temperature. Thus we start with the canonical partition function:

$$\mathcal{Z}(T) = \text{Tr} [e^{-\beta H}] = \text{Tr} [e^{-\beta(H_0 + \lambda V)}], \quad (\text{B1})$$

and seek to expand its logarithm in powers of λ . Since H_0 and V do not commute for the K- Γ model, we use the approach employed for interaction picture time evolution. We define the function $f(\beta)$ by:

$$e^{-\beta(H_0 + \lambda V)} = e^{-\beta H_0} f(\beta) \Rightarrow \frac{df(\beta)}{d\beta} = -\lambda e^{\beta H_0} V e^{-\beta H_0} f(\beta). \quad (\text{B2})$$

Casting this in the form of the integral equation, we get:

$$f(\beta) = 1 - \lambda \int_0^\beta d\tau \tilde{V}(\tau) f(\tau), \quad \tilde{V}(\tau) = e^{\tau H_0} V e^{-\tau H_0}, \quad (\text{B3})$$

which we solve by iteration:

$$f(\beta) = 1 + \sum_{n=1}^{\infty} (-\lambda)^n \int_0^{\beta} d\tau_1 \int_0^{\tau_1} d\tau_2 \cdots \int_0^{\tau_{n-1}} d\tau_n \tilde{V}(\tau_1) \tilde{V}(\tau_2) \cdots \tilde{V}(\tau_n). \quad (\text{B4})$$

This gives us the partition function as:

$$\mathcal{Z}(T) = \mathcal{Z}_0 \left[1 + \sum_{n=1}^{\infty} (-\lambda)^n \int_0^{\beta} d\tau_1 \int_0^{\tau_1} d\tau_2 \cdots \int_0^{\tau_{n-1}} d\tau_n \langle \tilde{V}(\tau_1) \tilde{V}(\tau_2) \cdots \tilde{V}(\tau_n) \rangle_0 \right], \quad (\text{B5})$$

where $\langle \cdots \rangle_0$ denotes the unperturbed expectation value:

$$\langle A \rangle_0 \equiv \frac{\text{Tr} [e^{-\beta H_0} A]}{\text{Tr} [e^{-\beta H_0}]} \quad (\text{B6})$$

for any operator A . The leading order term is given by:

$$\langle \tilde{V}(\tau) \rangle_0 = \frac{\text{Tr} [e^{-\beta H_0} e^{\tau H_0} V e^{-\tau H_0}]}{\text{Tr} [e^{-\beta H_0}]} = \frac{\text{Tr} [e^{-\beta H_0} V]}{\text{Tr} [e^{-\beta H_0}]}, \quad (\text{B7})$$

which is in fact independent of τ .

Let us compute the leading term in the partition function for the Hamiltonian of the main text, such that:

$$H_0 = - \sum_{\alpha=\{x,y,z\}} \tilde{B}_{\alpha} \sigma_j^{\alpha}, \quad V = \sum_{\gamma} \sum_{\langle jk \rangle_{\gamma-\text{links}}} J_{\alpha\beta}^{\gamma} \sigma_j^{\alpha} \sigma_k^{\beta}. \quad (\text{B8})$$

Hence, we get:

$$\langle \tilde{V}(\tau) \rangle_0 = \frac{\sum_{\gamma, \alpha', \lambda'} \sum_{\langle jl \rangle_{\gamma-\text{links}}} J_{\alpha'\lambda'}^{\gamma} \sinh(\beta \tilde{B}_{\alpha'}) \sinh(\beta \tilde{B}_{\lambda'})}{\cosh^2(\beta \tilde{B})} = \frac{N_c \sum_{\gamma, \alpha', \lambda'} J_{\alpha'\lambda'}^{\gamma} \sinh(\beta \tilde{B}_{\alpha'}) \sinh(\beta \tilde{B}_{\lambda'})}{\cosh^2(\beta \tilde{B})}, \quad (\text{B9})$$

where $\tilde{B} = \sqrt{\sum_{\alpha} \tilde{B}_{\alpha}^2}$, and N_c is the number of unit cells in the system. Finally, this gives us the partition function, corrected to leading order, as:

$$\mathcal{Z}(T) = \left[2 \cosh(\beta \tilde{B}) \right]^{2N_c} \left[1 + \beta N_c \sum_{\gamma, \alpha', \lambda'} J_{\alpha'\lambda'}^{\gamma} \frac{\sinh(\beta \tilde{B}_{\alpha'}) \sinh(\beta \tilde{B}_{\lambda'})}{\cosh^2(\beta \tilde{B})} \right]. \quad (\text{B10})$$

-
- [1] L. Balents, Spin liquids in frustrated magnets, *Nature* **464**, 199 (2010), DOI: 10.1038/nature08917.
- [2] L. Savary and L. Balents, Quantum spin liquids: a review, *Rep. Prog. Phys.* **80**, 016502 (2017), DOI: 10.1088/0034-4885/80/1/016502.
- [3] A. Kitaev, Anyons in an exactly solved model and beyond, *Annals of Physics* **321**, 2 (2006), DOI: 10.1016/j.aop.2005.10.005.
- [4] G. Jackeli and G. Khaliullin, Mott insulators in the strong spin-orbit coupling limit: From heisenberg to a quantum compass and kitaev models, *Phys. Rev. Lett.* **102**, 017205 (2009), DOI: 10.1103/PhysRevLett.102.017205.
- [5] J. G. Rau, E. K.-H. Lee, and H.-Y. Kee, Generic spin model for the honeycomb iridates beyond the kitaev limit, *Phys. Rev. Lett.* **112**, 077204 (2014), DOI: 10.1103/PhysRevLett.112.077204.
- [6] K. W. Plumb, J. P. Clancy, L. J. Sandilands, V. V. Shankar, Y. F. Hu, K. S. Burch, H.-Y. Kee, and Y.-J. Kim, $\alpha - \text{ruCl}_3$: A spin-orbit assisted mott insulator on a honeycomb lattice, *Phys. Rev. B* **90**, 041112 (2014), DOI: 10.1103/PhysRevB.90.041112.
- [7] S. M. Winter, Y. Li, H. O. Jeschke, and R. Valentí, Challenges in design of kitaev materials: Magnetic interactions from competing energy scales, *Phys. Rev. B* **93**, 214431 (2016), DOI: 10.1103/PhysRevB.93.214431.
- [8] S. Trebst, Kitaev materials, (2017), [arXiv:1701.07056 \[cond-mat.str-el\]](https://arxiv.org/abs/1701.07056).
- [9] R. Yadav, N. A. Bogdanov, V. M. Katukuri, S. Nishimoto, J. van den Brink, and L. Hozoi, Kitaev exchange and field-induced quantum spin-liquid states in honeycomb $\alpha\text{-ruCl}_3$, *Scientific Reports* **6**, 37925 (2016), DOI: 10.1038/srep37925.
- [10] Y. Sizyuk, P. Wölfle, and N. B. Perkins, Selection of direction of the ordered moments in na_2irO_3 and $\alpha - \text{ruCl}_3$, *Phys. Rev. B* **94**, 085109 (2016), DOI: 10.1103/PhysRevB.94.085109.
- [11] K. Riedl, Y. Li, S. M. Winter, and R. Valentí, Sawtooth torque in anisotropic $j_{\text{eff}} = 1/2$ magnets: Application to $\alpha\text{-ruCl}_3$, *Phys. Rev. Lett.* **122**, 197202 (2019), DOI: 10.1103/PhysRevLett.122.197202.
- [12] A. Banerjee, C. A. Bridges, J. Q. Yan, A. A. Aczel, L. Li, M. B. Stone, G. E. Granroth, M. D. Lumsden, Y. Yiu, J. Knolle, S. Bhattacharjee, D. L. Kovrizhin, R. Moessner, D. A. Tennant, D. G. Mandrus, and S. E. Nagler, Proximate Kitaev quantum spin liquid behaviour in a honeycomb magnet, *Nature Materials* **15**, 733 (2016), DOI: 10.1038/nmat4604.

- [13] A. Banerjee, P. Lampen-Kelley, J. Knolle, C. Balz, A. A. Aczel, B. Winn, Y. Liu, D. Pajerowski, J. Yan, C. A. Bridges, A. T. Savici, B. C. Chakoumakos, M. D. Lumsden, D. A. Tennant, R. Moessner, D. G. Mandrus, and S. E. Nagler, Excitations in the field-induced quantum spin liquid state of α - RuCl_3 , *npj Quantum Materials* **3**, 8 (2018), DOI: 10.1038/s41535-018-0079-2.
- [14] F. Lang, P. J. Baker, A. A. Haghighirad, Y. Li, D. Prabhakaran, R. Valentí, and S. J. Blundell, Unconventional magnetism on a honeycomb lattice in $\alpha - \text{rucl}_3$ studied by muon spin rotation, *Phys. Rev. B* **94**, 020407 (2016), DOI: 10.1103/PhysRevB.94.020407.
- [15] R. D. Johnson, S. C. Williams, A. A. Haghighirad, J. Singleton, V. Zapf, P. Manuel, I. I. Mazin, Y. Li, H. O. Jeschke, R. Valentí, and R. Coldea, Monoclinic crystal structure of $\alpha - \text{rucl}_3$ and the zigzag antiferromagnetic ground state, *Phys. Rev. B* **92**, 235119 (2015), DOI: 10.1103/PhysRevB.92.235119.
- [16] H.-S. Kim, V. S. V., A. Catuneanu, and H.-Y. Kee, Kitaev magnetism in honeycomb rucl_3 with intermediate spin-orbit coupling, *Phys. Rev. B* **91**, 241110 (2015), DOI: 10.1103/PhysRevB.91.241110.
- [17] S.-H. Do, S.-Y. Park, J. Yoshitake, J. Nasu, Y. Motome, Y. S. Kwon, D. T. Adroja, D. J. Voneshen, K. Kim, T. H. Jang, J. H. Park, K.-Y. Choi, and S. Ji, Majorana fermions in the Kitaev quantum spin system α - RuCl_3 , *Nature Physics* **13**, 1079 (2017), DOI: 10.1038/nphys4264.
- [18] I. A. Leahy, C. A. Pocs, P. E. Siegfried, D. Graf, S.-H. Do, K.-Y. Choi, B. Normand, and M. Lee, Anomalous thermal conductivity and magnetic torque response in the honeycomb magnet $\alpha - \text{rucl}_3$, *Phys. Rev. Lett.* **118**, 187203 (2017), DOI: 10.1103/PhysRevLett.118.187203.
- [19] T. Suzuki and S.-i. Suga, Effective model with strong kitaev interactions for $\alpha - \text{rucl}_3$, *Phys. Rev. B* **97**, 134424 (2018), DOI: 10.1103/PhysRevB.97.134424.
- [20] J. c. v. Chaloupka and G. Khaliullin, Magnetic anisotropy in the kitaev model systems na_2iro_3 and rucl_3 , *Phys. Rev. B* **94**, 064435 (2016), DOI: 10.1103/PhysRevB.94.064435.
- [21] K. A. Modic, R. D. McDonald, J. P. C. Ruff, M. D. Bachmann, Y. Lai, J. C. Palmstrom, D. Graf, M. K. Chan, F. F. Balakirev, J. B. Betts, and et al., Scale-invariant magnetic anisotropy in rucl_3 at high magnetic fields, *Nature Physics* **17**, 240–244 (2020), DOI: 10.1038/s41567-020-1028-0.
- [22] H.-S. Kim and H.-Y. Kee, Crystal structure and magnetism in $\alpha - \text{rucl}_3$: An ab initio study, *Phys. Rev. B* **93**, 155143 (2016), DOI: 10.1103/PhysRevB.93.155143.
- [23] J. Oitmaa, C. Hamer, and W. Zheng, *Series Expansion Methods for Strongly Interacting Lattice Models* (Cambridge University Press, 2006).
- [24] H. B. Cao, A. Banerjee, J.-Q. Yan, C. A. Bridges, M. D. Lumsden, D. G. Mandrus, D. A. Tennant, B. C. Chakoumakos, and S. E. Nagler, Low-temperature crystal and magnetic structure of $\alpha - \text{rucl}_3$, *Phys. Rev. B* **93**, 134423 (2016), DOI: 10.1103/PhysRevB.93.134423.
- [25] F. D. M. Haldane, Model for a quantum hall effect without landau levels: Condensed-matter realization of the “parity anomaly”, *Phys. Rev. Lett.* **61**, 2015 (1988), DOI: 10.1103/PhysRevLett.61.2015.
- [26] Private communications with Arkady Sekhter.
- [27] M. Majumder, M. Schmidt, H. Rosner, A. A. Tsirlin, H. Yasuoka, and M. Baenitz, Anisotropic $\text{ru}^{3+}4d^5$ magnetism in the $\alpha - \text{rucl}_3$ honeycomb system: Susceptibility, specific heat, and zero-field nmr, *Phys. Rev. B* **91**, 180401 (2015), DOI: 10.1103/PhysRevB.91.180401.